

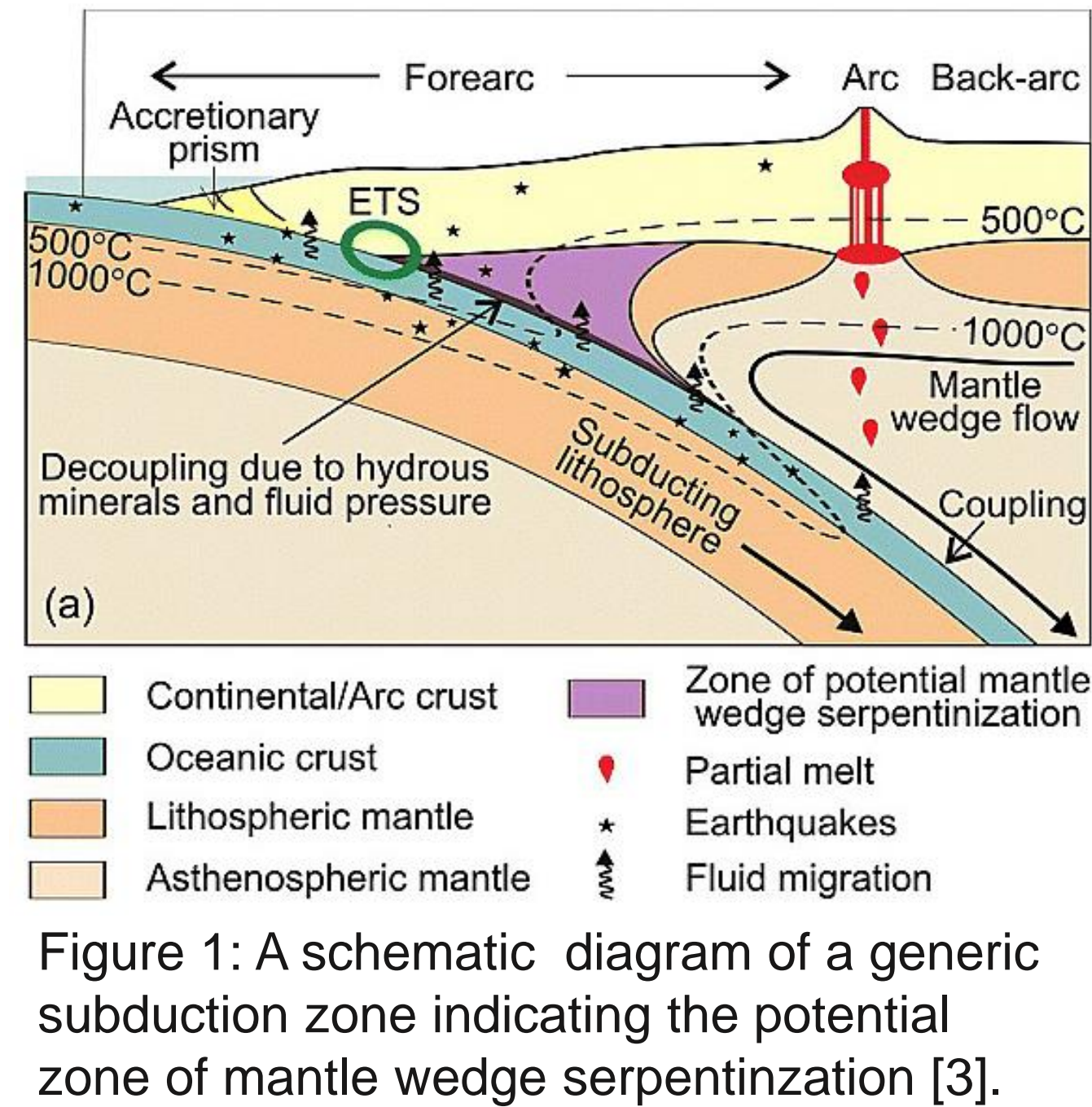
Effects of the Buoyancy of Serpentinized Mantle on Stresses in the Overriding Crust in Subduction Zones

Trey Brink & Ikuko Wada

Department of Earth Science, University of Minnesota

1. Introduction

Along a convergent plate boundary, the oceanic plate subducts beneath another plate, forming a complex tectonic environment, called a subduction zone. The mantle is present between these two plates and because of the shape, is known as the mantle wedge. The subducting slab hydrates the overriding mantle beneath the forearc region by releasing water that it absorbed while exposed to the ocean, which creates several hydrous minerals, the most abundant being serpentininite [1]. Serpentinite is less dense than the surrounding, relatively dry mantle, thus making the serpentinized mantle buoyant. This buoyancy affects the overall state of stress in the nearby regions and therefore the generation of earthquakes in the overlying forearc crust and along the plate interface. Therefore, quantifying the buoyancy effect of serpentinization is important to the studies of earthquake generation and seismic hazards.



2. Methods

To quantify the buoyancy effect of the serpentinized mantle wedge on crustal stresses we used PyLith, a numerical finite-element code for lithospheric deformation.

Figure 2.1: The mesh used in the model. The angled mesh is to account for the angle of subduction in future models.

PyLith solves the following equations of motion for displacement based on given initial and boundary conditions:

$$\rho \frac{\partial^2 u_i}{\partial t^2} - f_i - \sigma_{ij,j} = 0$$

where ρ , u , t , f_i , and $\sigma_{ij,j}$ are density (kg/m^3), displacement (m), time (s), body force vector ($\text{kg/m}^2/\text{s}^2$), and the divergence of the stress tensor (Pa/m), respectively. To simplify the problem, we exclude the effects of topography and subduction. We assume the mantle wedge is fully serpentinized, allowing us to see the buoyancy effect most easily.

Figure 2.2: The model set up in each of the three cases. A) Reference model with no low-density region, B) rectangular low-density region and, C) triangular low-density region. Density used for each region are noted on the figure.

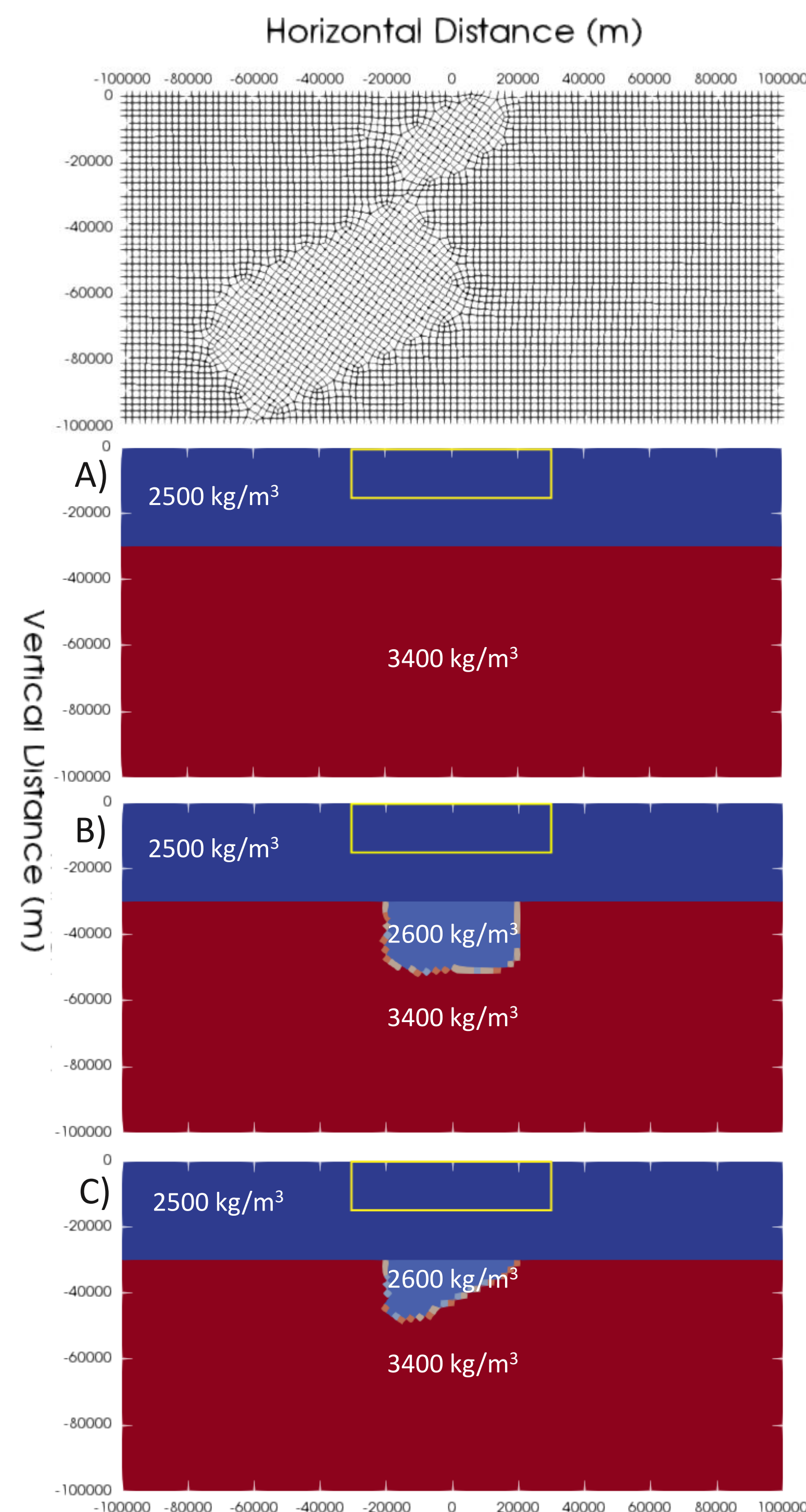


Table 2.1: Material properties used in the models.

	Viscoelastic Mantle	Low Density Region	Elastic Crust
Density (kg/m^3)	3400	2600	2500
Shear Modulus (GPa)	30.6	23.4	22.5
Lame's 1 st Parameter (GPa)	91.9	70.3	67.6
Dynamic Viscosity ($\text{Pa}\cdot\text{s}$)	2.3×10^{20}	2.3×10^{20}	

3. Results

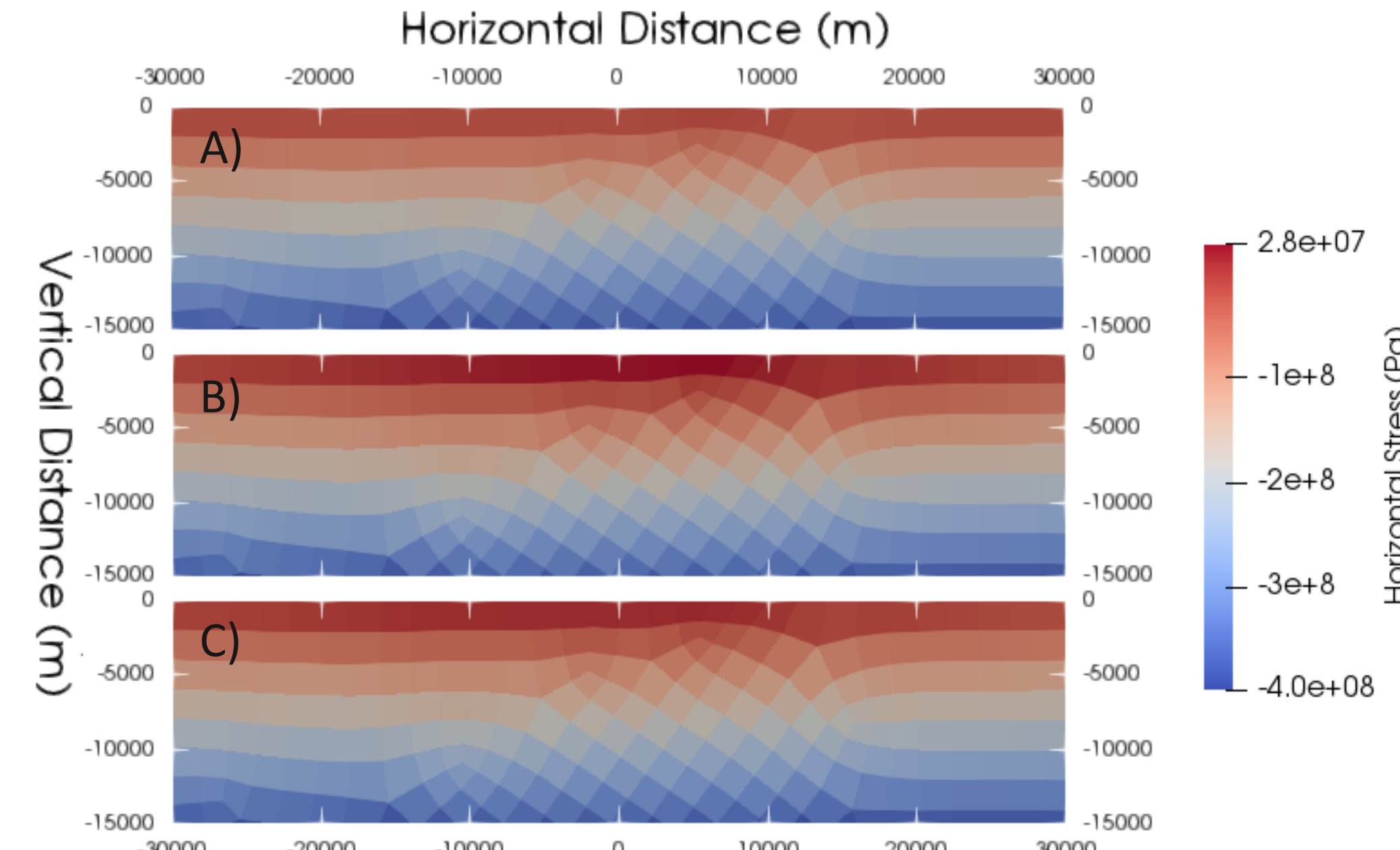


Figure 3.1: Horizontal stress variation within the yellow box shown in Figure 2.2.

Note that positive values indicate tensional stress. The reference model only experiences compressional stresses, while in both models with the low-density region tensional stresses are present in the shallow crust. The transition from compression to tension occurs at about 2 km depth in the rectangular model, and at about 1 km depth in the triangular model. However, these depths are imprecise due to the resolution of the model.

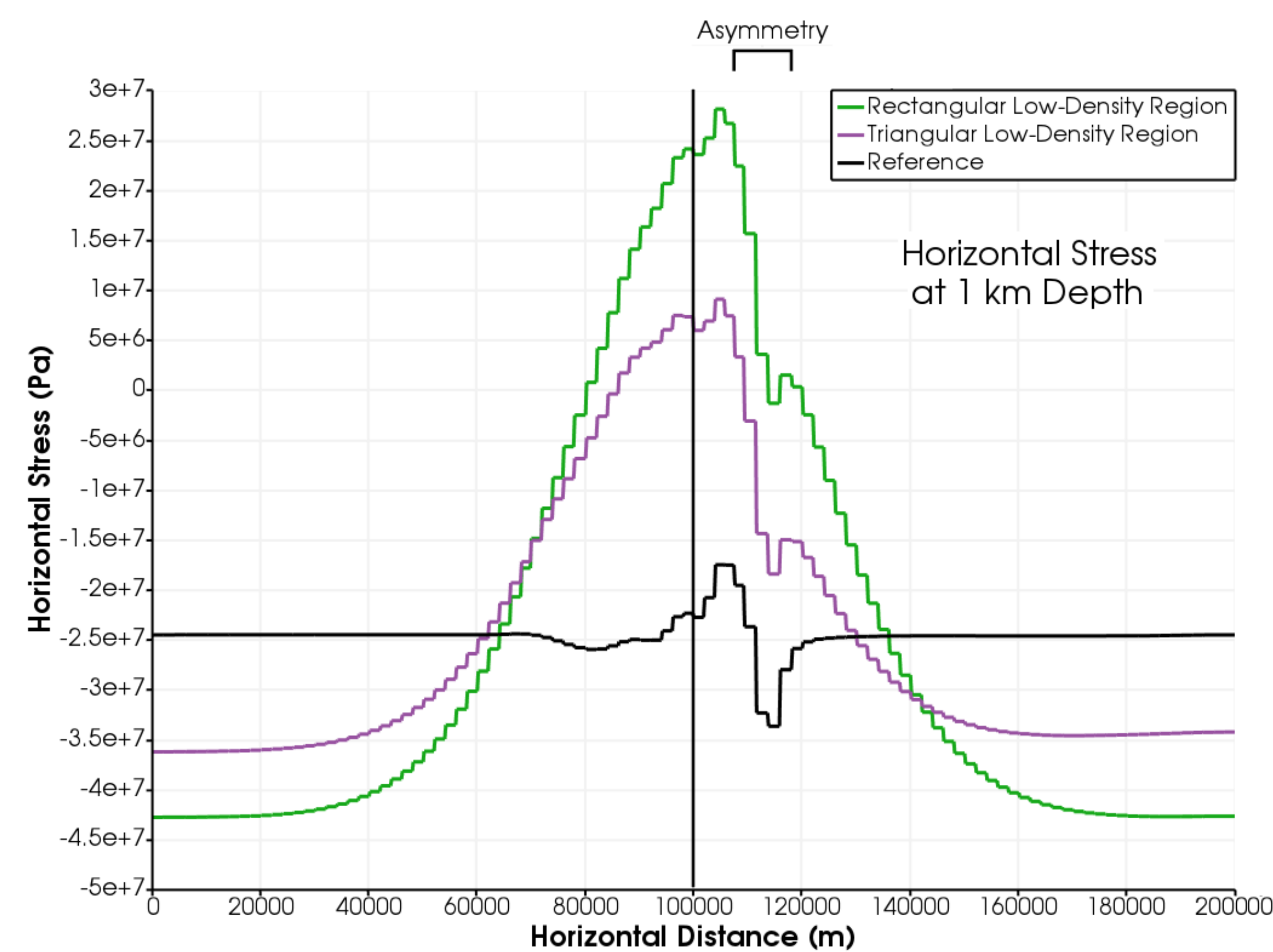


Figure 3.2: The horizontal stress profile at 1 km depth. The asymmetry is due to mesh construction.

The model with the rectangular low-density region indicates that a peak horizontal stress in the overlying crust occurs at the surface directly above the underlying low-density region, reaching 28 MPa. The model with the triangular region indicates a smaller peak horizontal stress of ~8 MPa. Both models with the low-density region also have greater compressional stresses beyond 40 km away from the center of the model. The drop in horizontal stress at about 115 km is the result of the angled mesh. The shift from tensional to compressional horizontal stresses occurs at 20 km away from the center in the rectangular low-density region, and 15 km away for the triangular low-density region. The triangular low-density region does shift the horizontal stress distribution slightly to the left side of the model, relative to the rectangular low-density region.

4. Discussion

The triangular region has roughly half the amount of buoyant material than the rectangular region, which is why the model indicates smaller tensile stresses in the overlying crust. However, our models use a mantle wedge that is fully serpentinized, while seismic observations indicate complete serpentinization is likely to occur only at the tip of the mantle wedge [2]. Therefore, the magnitudes of tensional stress in real systems are likely smaller than those predicted by our model.

The tensional stresses present in the shallow crust in our models are likely to promote the formation of extensional faults, and the distribution of earthquakes in the overlying crust can thus help to estimate the spatial extent and degree of serpentinization in the mantle wedge.

Further modeling could help to more precisely determine the effects of a serpentinized mantle wedge on overlying crustal stresses by using a less simplified model. For example, applying the subducting lithosphere's motion or incorporating the effects of back-arc spreading.

5. Conclusions

- A fully serpentinized mantle wedge induces tensional horizontal stresses in the overlying crust.
- These modeled tensional stresses promote the formation of normal faults in the shallow crust.
- The distribution of earthquakes in the overlying crust could be used to estimate the spatial extent and degree of serpentinization.

Acknowledgements

This project was supported by the University of Minnesota's Undergraduate Research Opportunities Program.

References

- Hyndman, R. D., & Peacock, S. M. (2003). Serpentinization of the forearc mantle. *Earth and Planetary Science Letters*, 212(3–4), 417–432.
- Wada, I., and K. Wang (2009), Common depth of slab-mantle decoupling: Reconciling diversity and uniformity of subduction zones, *Geochem. Geophys. Geosyst.*, 10, Q10009, doi:10.1029/2009GC002570.
- Carlson, R. L., and Miller, D. J. (2003), Mantle wedge water contents estimated from seismic velocities in partially serpentinized peridotites, *Geophys. Res. Lett.*, 30, 1250, doi:10.1029/2002GL016600, 5